Synthetic Anticancer Vaccine Candidates: Rational Design of Antigenic Peptide Mimetics That Activate Tumor-Specific T-Cells

Céline Douat-Casassus,[†,‡] Nathalie Marchand-Geneste,[‡] Elisabeth Diez,[§] Nadine Gervois,[§,▽] Francine Jotereau,*[,§,▽] and Stéphane Quideau*[,†,‡]

Institut Européen de Chimie et Biologie, 2 rue Robert Escarpit, 33607 Pessac Cedex, France, Institut des Sciences Moléculaires (UMR 5255 CNRS), Université Bordeaux 1, 351 cours de la Libération, 33405 Talence Cedex, France, INSERM, U601, 44093 Nantes, France, and Université de Nantes, 44322 Nantes, France

Received November 17, 2006

A rational design approach was followed to develop peptidomimetic analogues of a cytotoxic T-cell epitope capable of stimulating T-cell responses as strong as or stronger (heteroclytic) than those of parental antigenic peptides. The work described herein focused on structural alterations of the central amino acids of the melanoma tumor-associated antigenic peptide Melan-A/MART-1_{26-35} using nonpeptidic units. A screening was first realized in silico to select altered peptides potentially capable of fitting at the interface between the major histocompatibilty complex (MHC) class-I HLA-A2 molecule and T-cell receptors (TCRs). Two compounds appeared to be high-affinity ligands to the HLA-A2 molecule and stimulated several Melan-A/MART-1 specific T-cell clones. Most remarkably, one of them even managed to amplify the response of one clone. Together, these results indicate that central TCR-contact residues of antigenic peptides can be replaced by nonpeptidic motifs without loss of binding affinity to MHC class-I molecules and T-cell triggering capacity.

Introduction

Cytotoxic T-lymphocytes (CTL) play a major role in the immune defense against infections and tumors.[1,2] They recognize and kill, in the context of appropriate immune responses, target cells expressing ligands of their receptors (TCRs). These ligands are made of short (8−10 amino acids long) peptides that are derived from antigenic proteins through limited intracellular proteolysis. They are bound to MHC class-I molecules and are thus exposed at the target cell surface as peptide−MHC (pMHC) complexes.[3] The functional consequences of these TCR/pMHC interactions for T-cells are highly variable, ranging from full activation to inactivation, depending in part on the binding stability of the peptide to the MHC and, in a poorly understood manner, on the molecular recognition characteristics and kinetic aspects of the TCR interacting with the pMHC complex. TCR/peptide contacts are made primarily through the complementary-determining region 3 (CDR3) loops of the TCR, which exhibit the greatest degree of genetic variability.[4] Therefore, different TCRs interact in a different way with a given pMHC. The identification of antigenic peptides (APs) raised the hope that these TCR ligands could be used to stimulate specifically T-cell growth and function in vivo and hence to enhance protective immune responses.[5] This question was, in particular, addressed in the context of therapeutic cancer vaccine development. Yet, infusion of tumor APs to cancer patients, alone or in association with adjuvants, was so far poorly effective in inducing tumor specific T-cell expansion and tumor regression.[6] Tumor AP characteristics that could contribute to this lack of efficacy are: a limited antigenicity, revealed by the poor triggering of specific T-cell growth in vitro, and/or a short bioavailability due to high susceptibility to serum or tissue proteases.

Considerable efforts have therefore been done to derive epitope analogues of enhanced antigenicity or half-life in vivo. Because most tumor antigens are self-proteins, their limited antigenicity often results from central (intrathymic) tolerance mechanisms that eliminate the high-avidity self-specific TCR repertoire during T-cell development.[7] Therefore, the function of spared tumor associated antigen (TAA)-specific T-cells may remain poorly effective due to their limited avidity. In some cases, low avidity of TAA-specific T-cells result from the cognate AP exhibiting low affinity/stability for the self-MHC presenting molecule. The best known example of this is the Melan-A/MART-1_{26-35} AP expressed on the MHC class-I HLA-A2 molecule by most melanoma tumors.[8] In this case, amino acid substitutions enhancing HLA binding may provide peptide analogues of increased antigenicity capable of, at least some of them, efficiently triggering a T-cell repertoire that could cross-react with the natural peptide,[9] which is of course mandatory for vaccine use. High susceptibility to proteases, the other probable major cause of the limited in vivo antigenicity of APs in general and tumor APs in particular, can conceivably be counteracted by substituting standard α-amino acid residues by nonpeptidic groups. For example, previous attempts that were aimed at replacing *N*- and/or *C*-terminal residues to reduce AP susceptibility to amino- and carboxypeptidases succeeded in producing analogues with high-affinity binding to the MHC molecule and efficient TCR triggering.[10,11] Other studies addressed, also with some success, the compatibility of performing more central modifications of MHC-binding AP residues to increase AP binding affinity to the MHC pocket and, hence, T-cell reactivity.[12]

Another yet unexplored possibility is to substitute the central AP residues specifically interacting with the TCR by nonpeptidic motifs. Here we examined the feasibility of this approach, using as a model the aforementioned epitope of the melanoma-associated Melan-A/MART-1 antigen. The protein Melan-A/MART-1 (referred to as MART-1 hereafter) is a melanocyte lineage specific protein expressed in about 90% of primary and

* Address correspondence to either author. Phone: 33-540-00-2215. Fax: 33-540-00-2215. E-mail: s.quideau@iecb.u-bordeaux.fr (S.Q.); Phone: 33-240-08-4720. Fax: 33-240-08-4082. E-mail: jotereau@nantes.inserm.fr (F.J.).
[†] Institut Européen de Chimie et Biologie.
[‡] Institut des Sciences Moléculaires (UMR 5255 CNRS).
[§] INSERM.
[▽] Université de Nantes.

10.1021/jm0613368 CCC: $37.00
Published on Web 03/01/2007

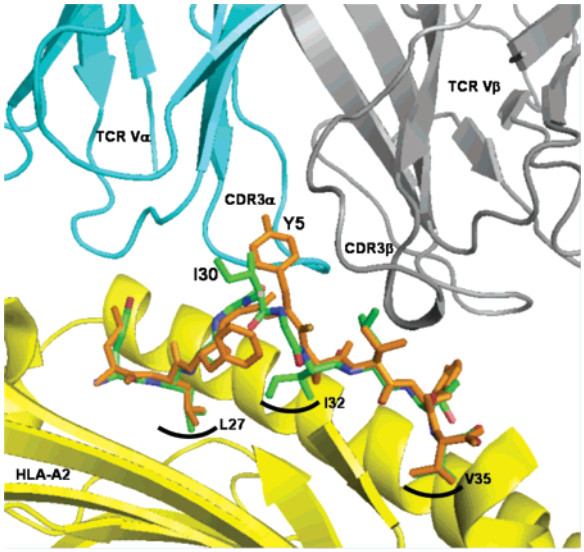

Figure 1. InsightII superimposition of the LigandFit-docked ELA peptide (green) in the Tax peptide (orange) binding site of the A6-TCR/HLA-A2 complex (PDB 1AO7). Positioning of main anchor residues [i.e., L27 (P2) and V35 (P10)] is almost identical to that of the Tax peptide with the ELA central region also bulging out from the center of the HLA-A2 binding domain toward the CDR3 TCR variable loops.

metastatic melanoma tumors.[13] MART-1-specific CTLs have been isolated from both peripheral blood mononuclear cells (PBMC) and tumor infiltrating lymphocytes (TILs) of HLA-A2 melanoma patients.[14,15] Later, the screening of peptides derived from MART-1 has permitted the identification of two APs: the nonapeptide AAGIGILTV (MART-1_{27-35}) and the decapeptide EAAGIGILTV (MART-1_{26-35}). More recently, it was reported that the MART-1_{26-35} decapeptide was better recognized by most tumor-reactive T-cells than the nonapeptide.[16] However, a drawback of both peptides was their low binding affinity to the HLA-A2 molecule. It is established that most human APs bind to MHC class-I molecules through 2 or 3 conserved anchoring residues, such as leucine at the 2-position in HLA-A2 binding APs.[17] Hence, synthetic analogues of the MART-1 epitopes having an alanine replaced by a leucine residue were produced and showed considerably increased HLA-A2 binding affinity (i.e., ALGIGILTV and ELAGIGILTV).[9] The ELAGIGILTV analogue was found to be more immunogenic than the natural peptide,[9] whereas ALGIGILTV was not recognized anymore by most Melan-A tumor-reactive CTL lines and clones. Drastic conformational differences were indeed observed between the central regions of the two bound peptides, and showed that the decapeptide ELAGIGILTV central region (i.e., GIG_{29-31}) adopts a "zigzag" structure, in which the hydrophobic I30 side chain bulges out from the center of the decamer.[18] Hence, the HLA-bound decapeptide would be better suited than its nonameric analogue to engage in more intimate contacts with TCRs (see Figure 1) for enhanced CTL activation. In any event, the heteroclytic properties observed in vitro for the modified decapeptide ELAGIGILTV led to its selection for vaccination clinical trials on melanoma patients.[19]

Such an AP analogue, however, still lacks acute immunogenicity. This disappointing clinical observation may be due again, at least in part, to the low stability of ELAGIGILTV in biological fluids.[3] Nevertheless, the considerable amount of work that has been performed on ELAGIGILTV both at the medicinal chemistry and clinical levels thus led us to select it as a first AP analogue model for developing our approach to nonpeptidic, potentially heteroclytic tumor-specific antigenic peptidomimetics based on the substitution of AP central TCR-contact amino acids by nonpeptidic moieties susceptible to interact efficiently with most TCRs. The crystallographic data available on the ELAGIGILTV/HLA-A2 binary complex[18] and others reported on TCR/AP/HLA-A2 ternary complexes,[20,21] as well as recent results reported by us and others,[22] all underlie the critical role played by hydrophobic structural elements on AP central regions in eliciting $CD8^+$ T-cell responses. In this article, we thus describe the rational design and synthesis approaches we followed with this premise in mind to generate novel and functional ELAGIGILTV-derived peptidomimetics.

Results and Discussion

Rational Design Strategy. The major difficulty encountered in the design of biologically active AP analogues is that their activity depends upon the accomplishment of two critical events: (1) binding to the MHC class-I molecule and (2) recognition by a TCR for signal triggering. To direct the design of our peptidomimetics, we relied on a shape-based docking engine, LigandFit from the Accelrys Cerius[2] software package (see Experimental Section).[23] Since no ternary complex structure involving ELAGIGILTV (referred to as ELA hereafter) has been reported as of today, we decided to base our docking studies on the 2.6 Å structure of the A6-TCR/Tax/HLA-A2 complex (PDB 1AO7, vide infra).[21] Notwithstanding the fact that the A6-TCR is not specific of ELA recognition, we surmised from literature data that conformations of any AP presented in the HLA-A2 binding groove would be quite similar.[24] The selected crystal structure shows that the HTLV-derived Tax AP (LLFGYPVYV) is oriented diagonally over the HLA-A2 molecule with the variable loops CDR1 and CDR3 of both Vα and Vβ TCR subunits contacting the peptide. The central Y residue protrudes out from the center of the HLA-A2 binding site and is completely surrounded by a deep and hydrophobic pocket delimited by the two TCR CDR3 loops (Figure 1). In order to gain some insights into the binding features of ELA into the HLA-A2 binding groove, while justifying the choice of the Tax-including ternary complex 1AO7 as the reference object for this study, we first docked ELA in place of the Tax peptide (Figure 1). The ELA conformation thus predicted is very similar to that of the Tax peptide with an almost perfect superimposition of their anchor residue side chains. Moreover, this docked conformation is quasi identical to that observed in the crystal structure of the ELA/HLA-A2 binary complex (PDB 1JF1).[18]

A virtual screening of several series of conceivable ELA analogues was then achieved using the LigandFit program before considering their synthesis. Every first proposed docked conformation (having the best docked energy) was compared to that of ELA by superimposition in Insight II again using 1AO7 structure as the reference object. Since the activity of a given AP essentially depends on its docked structure in the ternary complex, three main checkpoints were chosen as a mean of selecting the most appropriate central region modifications: (1) orientation of anchor residues (L2 and V10); (2) conservation of peptide backbone folding; (3) orientation of putative TCR-contact side chains. One of the benefits of this analysis in silico was to gain diagnostic structural information to guide our peptidic backbone modifications toward a better targeting of the TCR binding groove. Different generations of ELA analogues were iteratively designed from the simplest ones, bearing only different α-amino acid residues in their central region, to peptidomimetics in which standard peptidic features were gradually eliminated.

Table 1. HLA-A2 Binding Affinities of the 23 ELA Analogues

compd	sequence[a]	R group	RFI ratio[b]
ELA	ELAGIGILTV		1.0
EAA	EAAGIGILTV		0.63
1	ELAGYGILTV		0.80
2	ELAGFGILTV		0.97
3	ELAGWGILTV		0.73
4	ELAG(ΨCH$_2$NH)YG(ΨCH$_2$NH)ILTV		1.71
5	ELAG(ΨCH$_2$NH)WG(ΨCH$_2$NH)ILTV		1.61
6	ELAG(ΨCH$_2$NH)W-Amba-LTV		1.34
7	ELA-NH-(CH$_2$)$_2$-(R)G-GILTV	CH$_2$-C$_6$H$_4$-NO$_2$	0.85
8	ELA-NH-(CH$_2$)$_2$-(R)G-GILTV	CH$_2$-C$_6$H$_5$	0.90
9	ELA-NH-(CH$_2$)$_2$-(R)G-GILTV	CH$_2$-naphtalene	0.70
10	ELA-NH-(CH$_2$)$_2$-(R)G-GILTV	CH$_2$-quinoline	0.79
11	ELA-NH-(CH$_2$)$_2$-(R)G-GILTV	CH$_2$-C$_6$H$_4$-OH	0.83
12	ELA-NH-(CH$_2$)$_2$-(R)G-GILTV	CH$_2$-C$_6$H$_{11}$	0.86
13	βALA-NH-(CH$_2$)$_2$-(R)G-GILTV	CH$_2$-C$_6$H$_5$	0.96
14	βALA-NH-(CH$_2$)$_2$-(R)G-Amba-LTV	CH$_2$-C$_6$H$_4$-NO$_2$	0.86
15	βALA-NH-(CH$_2$)$_2$-(R)G-Amba-LTV	CH$_2$-quinoline	1.31
16	βALA-NH-(CH$_2$)$_2$-(R)G-Amba-LTV	CH$_2$-C$_6$H$_5$	0.95
17	βALA-NH-(CH$_2$)$_2$-(R)G-Amba-LTV	(CH$_2$)$_2$-C$_6$H$_5$	0.25
18	βALA-NH-(CH$_2$)$_2$-(R)G-Amba-LTV	(CH$_2$)$_2$-indole	0.86
19	βALA-NH-(CH$_2$)$_2$-(R)G-Amba-LTV	(CH$_2$)$_2$-C$_6$H$_4$-OH	0.42
20	βALA-NH-(CH$_2$)$_2$-(R)G-Amba-LTV	CO-CH$_2$-C$_6$H$_5$	0.54
21	βALA-NH-(CH$_2$)$_2$-(R)G-Amba-LTV	CO-CH$_2$-indole	1.02
22	βALA-G(ΨCH$_2$NH)Tpi-Amba-LTV		0.81
23	βALA-G(ΨCH$_2$NH)Tic-Amba-LTV		0.64

[a] For chemical structures, see Schemes 1 and 2 and Supporting Information. [b] Normalized HLA-A2 binding affinities of ELA analogues relative to that of ELA expressed as relative fluorescence intensities (RFI).

Scheme 1. Structural Representation of the Synthesized ELA Mimetics of First and Second Generations[a]

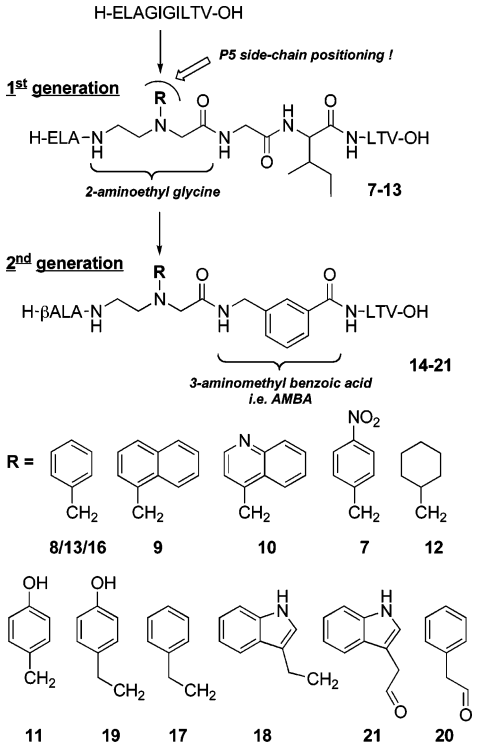

[a] NB: for **13**, the *N*-terminal glutamic acid (E) residue was replaced by a *β*-alanine residue (see text and Table 1).

Generation and HLA-A2 Binding Affinity of ELA Analogues. Thus, our preliminary modifications of ELA were simply based on the substitution of I30 (P5) by aromatic amino acids in the aim of assessing the role played by central aromatic pegs in the HLA-A2-restricted AP recognition process by TCRs. Three peptides having Y, F, or W at P5 (**1**−**3**, Table 1) were synthesized and assayed for their capacity to maintain binding to the HLA-A2 molecule. All three bind with a relative affinity comparable to that of ELA, but better than that of EAA, the natural antigenic peptide.

The introduction of functional spacers was then envisioned in the ELA central region. To mimic the central tetrapeptidic fragment GIGI (P4−P7), nonpeptidic spacer needs to reproduce as closely as possible the conformation of this central "zigzag" region, while allowing adequate orientation of the anchor residues L2 and V10. This is the reason why we initially decreased as little as possible the central peptide features and worked our way up stepwise to more drastic structural changes. The first classical backbone modification implemented was the introduction of reduced peptide bonds.[25] Notwithstanding previous studies that have shown that such alterations are often detrimental to the binding affinity to the MHC class-I molecules,[26] not only one but two of these reduced bonds were envisaged between each glycine residue and its right-adjacent residue in peptides **1** and **3** to give **4** and **5** (Table 1). Docking of the corresponding altered peptides in the A6-TCR/Tax/HLA-A2 complex indicated backbone geometries similar to that of the ELA peptide. These two modified ELA peptides **4** and **5** were then synthesized and evaluated for their HLA-A2 binding affinity. Strikingly, they turned out to be better ligands than the ELA peptide, showing a 2-fold increase in relative affinity as compared to that of the natural antigenic peptide EAA (Table 1).

Since the incorporation of 1,2-diaminoethyl units (i.e., reduced G residue) in the peptide backbone was found to have a positive influence on binding affinity to the HLA-A2 molecule, we thought of pursuing our modification by replacing the dipeptide GI$_{29,30}$ by such a type of spacer and exploiting the secondary amine function to attach various organic motifs that could mimic the central TCR-oriented side chain functionalities of the natural aromatic amino acids F, Y, and W used in peptides **1**−**5**. We were further inclined to do so on the basis of previous studies that have shown that the central part of an AP can be replaced either by poly-*N*-acylated amines or by aliphatic spacers without loss of binding affinity to MHC molecules.[12,27] Among the various spacers we considered, *N*-(2-aminoethyl)glycine, which is classically used in peptide nucleic acid chemistry,[28] was identified as the unit responding the best to the structural criteria imposed by the docking procedure, the most important of which being the positioning of the central tether in the same vicinity as the side chain of ordinary residues at P5 (Scheme 1, first generation). When this spacer, bearing different organic motifs, was introduced in the peptide sequence in place of GI$_{29,30}$, the resulting altered peptides **7**−**12** displayed docked conformations similar to that of ELA. The L2 and V10 anchor side chains were positioned as in ELA, and the modified central parts bulged out of the HLA-A2 binding groove, hence presenting their organic tether toward the CDR3α loop of the TCR (not shown). An analogue of the *N*-benzylated construct **8** (i.e., **13**, Table 1) was also made by replacing its *N*-terminal glutamic acid (E) residue by a *β*-alanine residue, for such a modification of the ELA *N*-terminus has been shown to render the molecule much more resistant to peptidase-mediated degradation.[10,29] The seven pseudo-peptides of this series (i.e., **7**−**13**) expressed affinities to the HLA-A2 molecule at a level comparable to that of the ELA peptide (Table 1). Moreover, the presence of the *N*-terminal *β*-alanine in **13** did not alter its HLA-A2 binding affinity (Table 1). Again, all of these pseudo-peptides were of course much better ligands than the natural antigenic peptide EAA (Table 1).

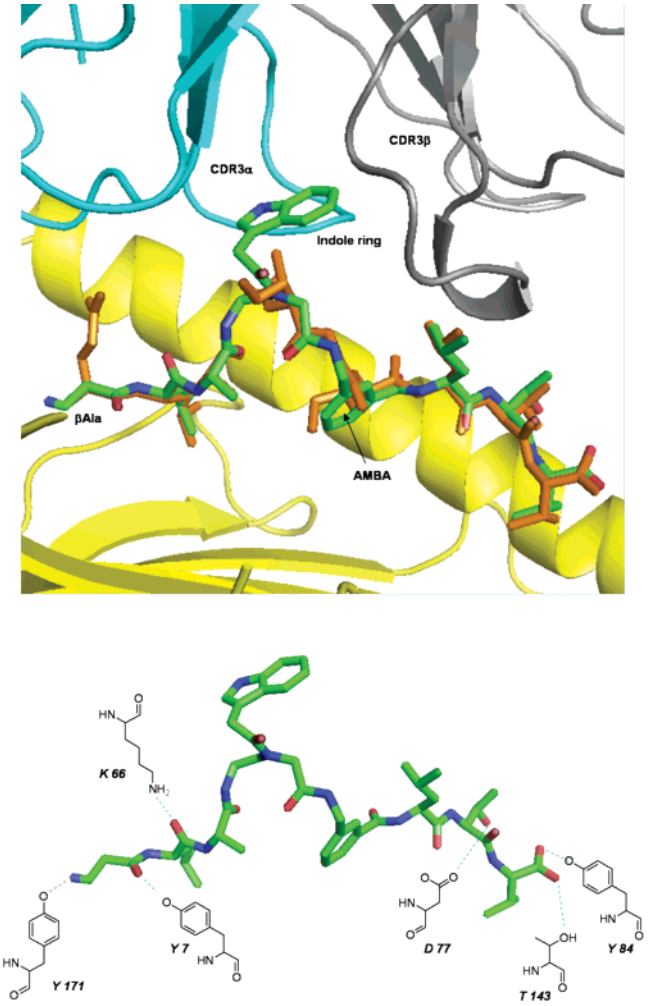

Figure 2. LigandFit docking of ELA and its mimetic **21** in the A6-TCR/Tax/HLA-A2 complex. Top: InsightII superimposition of **21** (green) and ELA (orange) after docking in the Tax binding site; the CDR3-α loop is in blue, the CDR3-*β* is in gray, and the MHC class-I HLA-A2 molecule is in yellow. Bottom: InsightII representation of the H-bonding network between **21** and the HLA-A2 molecule.

In addition to this spacer, the replacement of the second $GI_{31,32}$ was envisaged. For the sake of simplicity of synthesis, commonly used building blocks were screened. Among the different hydrophobic dipeptide mimetics described in the literature and commercially available,[30] the only one that gave satisfactory docking results was the 3-aminomethyl benzoic acid (AMBA, see Scheme 1, second generation). When AMBA was thus introduced in place of $GI_{31,32}$, the peptide backbone folding in the HLA-A2 binding cleft was unchanged. Remarkably, the phenyl ring of AMBA was oriented in a manner similar to that of the I32 side chain at P7 (see AMBA positioning in Figure 2), filling the hydrophobic HLA-A2 pocket with no perturbation of the positioning of the main anchor residue side chains at P2 and P10. This AMBA spacer was thus combined either with a reduced peptide bond at P4 (i.e., **6**, Table 1) or with the *N*-(2-aminoethyl)glycine at P4 and P5. In this later case, the *N*-terminal glutamic acid residue was also replaced by a *β*-alanine residue (vide supra). A second generation of eight peptidomimetics was thus synthesized and evaluated for their binding affinity to the HLA-A2 molecule (i.e., **14**−**21**, Table 1 and Scheme 1). In this series, the length of the central aromatic tether was also increased by one carbon member either as a methylene unit (i.e., **17**−**19**) or as a carbonyl unit (i.e., **20**−**21**). These homologations were made in the aim of enabling

Scheme 2. Examples of ELA Mimetics of Third Generation

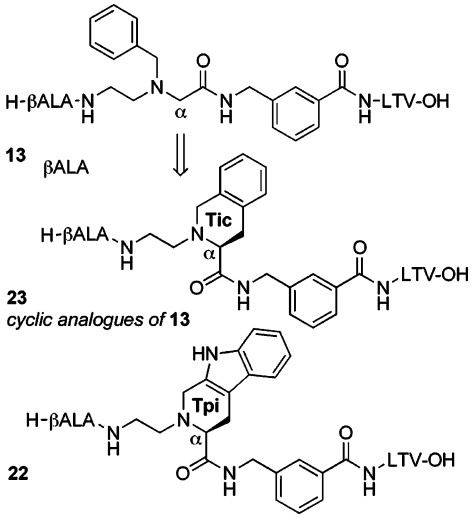

these ELA mimetics to penetrate deeper in between the TCR CDR3 loops.[22e] Such transformations were found to be highly detrimental to the binding affinity to the HLA-A2 molecule, except for the indole-bearing compounds (see RFI values for **17** and **19**−**20** vs **18** and **21** in Table 1). The docking in the A6-TCR/Tax/HLA-A2 complex structure of the indole-bearing construct **21** illustrates particularly well the adequacy of the modifications made on ELA, as it shows an overall backbone conformation and a hydrogen bonding connection with the HLA-A2 molecule identical to those of the ELA peptide (Figure 2). Both ELA and **21** express the same level of binding affinity to the HLA-A2 molecule (Table 1).

The satisfactory level of HLA-A2 affinity observed with the AMBA-containing compounds of second generation led us to examine an additional type of transformation aimed at rigidifying the peptidomimetic backbone, while fixing the orientation of central aromatic motifs toward the hydrophobic cavity of the TCR CDR3 loops. In agreement with the results of our in silico docking analysis, two additional analogues were thus envisaged bearing either the cyclic Phe mimic *N*-Fmoc-L-tetrahydroisoquinoline-3-carboxylic acid (i.e., **Tic**)[31] or the cyclic Trp mimic *N*-Fmoc-L-tetrahydronorharman-3-carboxylic acid (**Tpi**)[32] in place of the first GI fragment. These building blocks were coupled to a reduced glycine residue at P4 to constitute Cα-cyclized variants of the *N*-(2-aminoethyl)glycine spacer. This last series of AMBA-containing ELA mimetics again featured a bioresistant *β*-alanine residue at P1 (i.e., **22** and **23**, Table 1 and Scheme 2). Unfortunately, these modifications did not lead to any improvement of the binding affinity to the HLA-A2 molecule (Table 1).

Overall, our binding affinity results demonstrate that the central GIGI part of ELA can be replaced by nonpeptidic elements on which can be attached various organic motifs without drastic changes in binding affinity to the HLA-A2 molecule. It is admittedly difficult to predict each time the affinity behavior of a given peptidomimetic from its docking in silico using the LigandFit protocol. All designed ELA mimetics do not experimentally respond to the expectations drawn from the preliminary docking analysis, but all peptidomimetics having a high affinity to the HLA-A2 molecule feature structural modifications that were shown by LigandFit to allow docking in between the HLA-A2 and the TCR molecules in a manner similar to that of the starting peptide ELA. Thus, the LigandFit program constitutes a valuable tool to screen potential peptidomimetic structures prior to their synthesis.

Scheme 3. Solid-Phase Synthesis of Peptidomimetics **7**−**10** and **12**/**13** and the AMBA-Containing Peptidomimetics **14**−**17**[a]

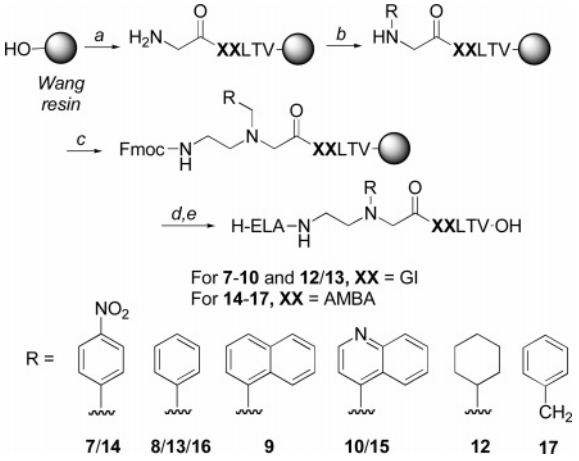

[a] Key: (a) standard SPPS; (b) RCHO (0.25 M), 2% AcOH−DCE, 2 h, filtration, $NaBH(OAc)_3$, DCE, 3 h; (c) Fmoc-Gly-H, $NaBH_3CN$, 1% AcOH−DMF, 10 h; (d) SPPS; (e) final deprotection and cleavage from resin, TFA−TIS−H_2O (95:2.5:2.5). NB: *t*-butyl protecting groups on Thr (T) and Glu (E) side chains are omitted for clarity; for **13** to **17**, the *N*-terminal glutamic acid (E) residue was replaced by a *β*-alanine residue (see text).

Scheme 4. Synthesis of *N*-Fmoc-*N*-(2-Aloc)-aminoethylglycine **27** and Peptidomimetic **11**[a]

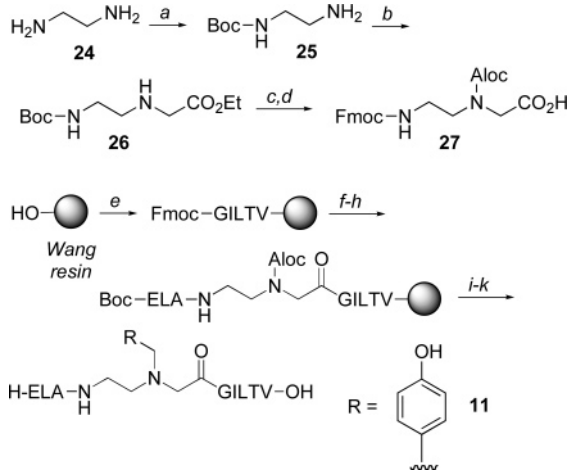

[a] Keys: (a) Boc_2O, THF, 0 °C, 95%; (b) $BrCH_2CO_2Et$, TEA, THF, 56%; (c) (i) Aloc-Cl, Na_2CO_3, H_2O, dioxane, (ii) LiOH, H_2O, 76%; (d) (i) TFA, (ii) Fmoc-OSu, NaOH, H_2O, CH_3CN, 91%; (e) SPPS; (f) 20% piperidine−DMF; (g) **27**, HBTU, DIEA, DMF; (h) SPPS; (i) $Pd(PPh_3)_4$, $PhSiH_3$, DCM; (j) RCHO (i.e., hydroxybenzaldehyde), $NaBH_3CN$, 1% AcOH−DMF, 10 h; (k) final deprotection and cleavage from resin, TFA−TIS−H_2O (95:2.5:2.5).

Chemical Synthesis. All modified peptides and peptidomimetics **1**−**23** (Table 1) were manually prepared via classical solid-phase peptide synthesis (SPPS) on a Wang resin using the Fmoc/*t*-butyl strategy. *N*-Fmoc-protected amino acids were condensed using HBTU[a] and DIEA as coupling agents in DMF for 45 min. *N*-Fmoc deprotections were carried out in 4:1 DMF−piperidine solvent mixture. The *N*-terminal residue was introduced as an *N*-Boc-protected amino acid. All compounds were then simultaneously cleaved from the resin and fully deprotected by the addition of TFA in the presence of TIS and water (EDT was added to this cleavage cocktail in the case of the indole-containing compounds **18** and **21**). Purification of all compounds was accomplished by semipreparative RP-HPLC, and their identification was carried out by positive-mode electrospray ionization (ESI) mass spectrometry (MS) (see Table 1, Experimental Section and Supporting Information).

The synthesis of the peptide analogues containing reduced peptide bonds (Table 1, **4**−**6**) required a reductive amination between the *N*-α-amino function of the peptide fragments anchored to the resin and *N*-Fmoc-glycinal (i.e., Fmoc-Gly-H), preliminary generated in solution by reduction of its corresponding morpholine amide using $LiAlH_4$.[33] Reduction of the imine intermediate was carried out using $NaBH_3CN$ in DMF containing 1% (v/v) of AcOH.[25] This procedure was also applied to the synthesis of the rigidified peptidomimetics **22** and **23** (Table 1 and Scheme 2). These peptides were obtained in satisfactory yields (54−68%) and purities, after purification by semipreparative RP-HPLC (see Experimental Section and Supporting Information, Table S1).

Four different strategies were followed for the synthesis of ELA mimetics of first and second generations (Schemes 3−6). For incorporation of *N*-linked central side chains (RCH_2−) that are nonsensitive to the SPPS conditions used (Scheme 3), a first reductive amination was performed between the free *N*-terminal α-amino function of the glycinyl residue of the fragments anchored to the resin and the corresponding aldehyde RCHO using $NaBH(OAc)_3$ as reducing agent.[34] The resulting secondary amine was then subjected to a second reductive amination reaction with Fmoc-Gly-H using $NaBH_3CN$ as reducing agent.[27] Following condensation with the *N*-terminal ELA or *β*-ALA (i.e., for **13**−**17**) fragment, final deprotection, and cleavage from the resin, the peptidomimetics **7**−**10** and **12**−**17** were obtained in yields ranging from 27 to 55%, after semipreparative RP-HPLC purification (see Experimental Section and Supporting Information, Table S1).

The second strategy consisted in preparing first the entire peptide sequence using the required amino acid building blocks and the *N*-Fmoc-*N*-(2-Aloc)-aminoethylglycine spacer **27**, the synthesis of which is depicted in Scheme 4, and then in attaching any organic side chain after release of the Aloc-protected secondary amine. This strategy was thought to be advantageous when using aldehydes RCHO bearing a second function sensitive to SPPS conditions, for they could thus potentially be attached via reductive amination as an unprotected entity just before the release of the construct from the support. This turned out to be successful only for the attachment of the 4-hydroxybenzaldehyde (Scheme 4), which led to the formation of the first-generation construct **11** in a yield of 46%, after RP-HPLC purification (see Experimental Section and Supporting Information, Table S1). All attempts to introduce the *N*-unprotected 3-formylindole group by this approach failed.

The third strategy was based on an approach previously used for peptoid synthesis[35,36] and was applied here for the synthesis of the second-generation AMBA-containing peptidomimetics **18** and **19**, for which central side chains (RCH_2−) could be attached as free primary amines via nucleophilic substitution reactions. Bromoacetic acid served to introduce the complementary electrophilic function and was directly condensed with the AMBA amino group of the solid-supported peptidomimetic precursor (Scheme 5). The resulting α-bromo acetyl amide **28** was then reacted with either N^{in}-Boc-tryptamine (**29**)[37] or *O*-*t*Butyramine (**30**),[38] and each product was submitted to reductive amination with Fmoc-Gly-H as before. Completion of the synthesis via SPPS furnished the desired peptidomimetics **18**

[a] Abbreviations: HBTU, 2-(1*H*-benzotriazol-1-yl)-1,1,3,3-tetramethyluroniumhexafluorophosphate; DIEA, *N*,*N*′-diisopropylethylamine; DMF, dimethylformamide; DCE, 1,2-dichloroethane, DIC, 1,3-di-*iso*-propylcarbodiimide; TFA, trifluoroacetic acid; TIS, triisopropylsilane; EDT, ethanedithiol.

Scheme 5. Synthesis of AMBA-containing Peptidomimetics **18** and **19**[a]

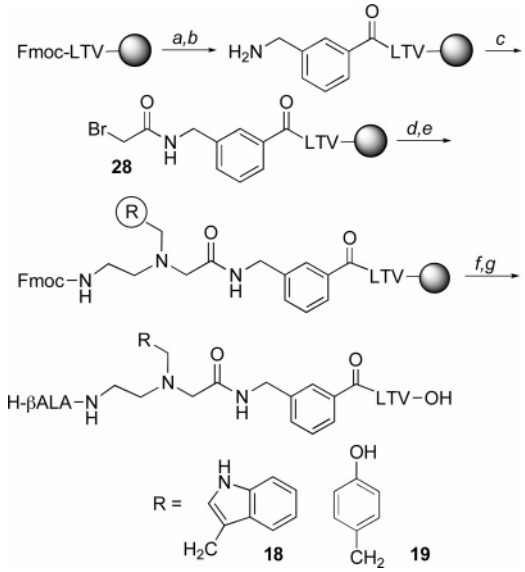

[a] Keys: (a) Fmoc-AMBA-OH, HBTU, DIEA, DMF; (b) 20% piperidine−DMF; (c) bromoacetic acid (0.4 M), DIC (2 M), DMF, 5 min, rt; (d) **29** or **30**, DMSO (see text); (e) Fmoc-Gly-H, $NaBH_3CN$, 1% AcOH−DMF, 10 h; (f) SPPS; (g) final deprotection and cleavage from resin using TFA−EDT−TIS−H_2O (92.5:2.5:2.5:2.5) for **18** and TFA−TIS−H_2O (95:2.5:2.5) for **19**.

Scheme 6. Synthesis of AMBA-Containing Peptidomimetics **20** and **21**[a]

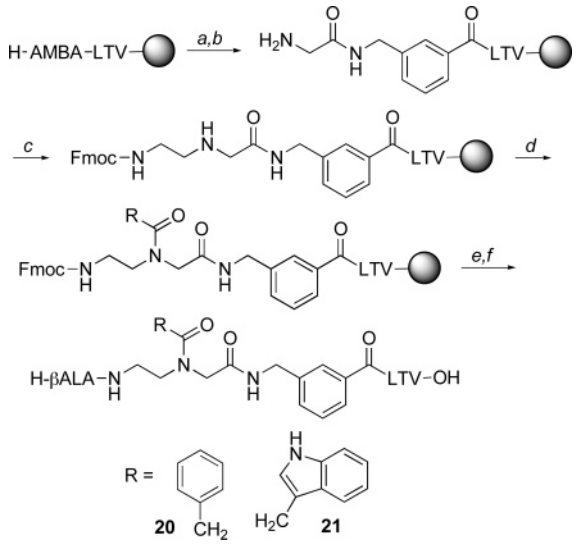

[a] Keys: (a) Fmoc-Gly-OH, HBTU, DIEA, DMF; (b) 20% piperidine−DMF; (c) Fmoc-Gly-H, $NaBH_3CN$, 1% AcOH−DMF, 10 h; (d) **31** or **32** (see text), DIC, DMF; (e) SPPS; (f) final deprotection and cleavage from resin using TFA−TIS−H_2O (95:2.5:2.5) for **20** and TFA−EDT−TIS−H_2O (92.5:2.5:2.5:2.5) for **21**.

and **19** in satisfactory yields and purities (see Experimental Section and Supporting Information, Table S1).

The last strategy was followed to build peptidomimetics **20** and **21** bearing side chains acylated to the *N*-(2-aminoethyl)-glycine spacer. To the *N*-terminal amino group of their AMBA-containing peptidomimetic precursor was successively attached Fmoc-Gly-OH via standard SPPS coupling and Fmoc-Gly-H via reductive amination (Scheme 6). The resulting free secondary amine function was then acylated with either phenylacetic acid (**31**) or indolacetic acid (**32**) using DIC in DMF. Completion of the synthesis via SPPS furnished the desired peptidomimetics **20** and **21** in satisfactory yields and purities (see Experimental Section and Supporting Information, Table S1).

T-Cell Recognition. All 23 modified ELA peptides and peptidomimetics were assayed for their capacity to stimulate a panel of seven different Melan-A-specific T-cell clones (expressing different TCR Vβ segments) previously obtained from melanoma infiltrating T-cells (TILs) or from peptide-stimulated PBLs. HLA-$A2^+$ human mutant T2 cells pulsed with each of the 23 compounds in 10 μM solutions were used to stimulate T-cell clones (see Experimental Section). Both the natural MART-1_{26-35} epitope EAA, naturally expressed by tumor cells, and its analogue ELA were used as positive controls. Since the 23 ELA analogues and mimetics were synthesized at different periods of our investigation, they were assayed in two separate series of experiments (Table 2). Their capacity to induce T-cell responses was evaluated by determining the fraction of clone cells producing IFN-γ by intracellular labeling. Cytokine production by CTL clones correlates with the level of TCR engagement and intracellular cytokine labeling of the fraction of activated T-cells clones provides a fine quantitative assessment of the relative T-cell activation.[39] Results obtained with all T-cell-stimulating antigenic peptide analogues and peptidomimetics are reported in Table 2 and are compared with responses obtained in the same experiment with the control peptides EAA and ELA. The simple replacement of the TCR-contacting I residue at P5 by Y, F, or W (i.e., peptides **1**−**3**) resulted in full conservation of the recognition by several T-cell clones. All three peptides stimulated the same four clones, although at a different level, and one (i.e., **3**) also activated another clone (M77.84). Therefore, the nature of the aromatic residue thus introduced at P5 of the ELA sequence influences both the specificity and the level of T-cell recognition. These first results confirmed those of previous studies showing that the introduction of an aromatic side chain at the center of the ELA sequence was not detrimental to its recognition by TCRs, even though the corresponding peptides were not as good HLA-A2 ligands as ELA (Table 1).[22d] The next and first series of pseudo-peptides (i.e., **4**−**6**), still bearing the same types of central aromatic amino acid residues (i.e., Y or W) was credited with a high potential for efficient T-cell stimulation, because of their high relative binding affinity to the HLA-A2 molecule (Table 1). We were then obviously disappointed by the total lack of activity of the two doubly reduced peptide analogues **4** and **5**. However, the replacement of the second reduced GI fragment of **5** by the AMBA unit led to the high-affinity ligand **6** that was capable of stimulating four different Melan-A-specific CTL clones with similar efficacy than the ELA peptide. Indeed, **6** induced a response quite similar to that of ELA for two clones (MEL1-37 and M17.29 ELA1) and slightly lower for two others (M199.2.7 and CDM41.ELA1) (Table 2, second series).

These last and very encouraging results prompted us to know whether or not our more drastically modified ELA mimetics of first, second, and/or third generations could mimic as well the activity of the ELA peptide. Among the 17 compounds of these series (i.e., **7**−**23**), it is another AMBA-containing structure that revealed itself as a particularly interesting construct. This peptidomimetic **21** features four modifications of the starting ELA peptide sequence. The *N*-terminal residue has been replaced by a β-alanine, the first GI fragment by the *N*-(2-aminoethyl)glycine spacer, the side chain of the central isoleucine residue at P5 by a *N*-carbonylmethylene-linked indole, and the second GI fragment by the AMBA unit. Gratifyingly, this heavily modified structure turned out to be the best elicitor of IFN-γ secretion, as it stimulated at significant levels four out

Table 2. IFN-γ Production of T-Cell Clones after Stimulation by T2 Cells Pulsed with Different ELA-Derived Peptides and Mimetics[a]

First Series

compd	M77.84	M199.2.7	M199.3.2	MEL1.37	CDM41 ELA1	M17.29 ELA1	10C10
EAA	87	41	85	83	73	75	50
ELA	90	38	88	86	77	65	71
1	4	0	**78**	**84**	**63**	**32**	0
2	32	7	**83**	**71**	**58**	**48**	
3	**90**	15	**54**	**81**	**47**	**55**	0
7	0	0	0	0	**64**	0	0
10	0	0	0	3	**69**	0	0
11	0	0	0	0	**46**	0	0

Second Series

compd	M77.84	M199.2.7	MEL1.38	MEL1.37	CDM41	M17.29	10C10
EAA	40	27	80	82	35	76	60
ELA	53	30	86	84	33	78	76
6	0	**22**	26	**82**	**28**	**84**	0
21	12	**25**	**44**	**89**	**31**	**27**	0

[a] Results are expressed as percentages of IFN-γ producing cells measured by flow cytometry upon intracellular IFN-γ labeling (see Figure 4 and Experimental Section).

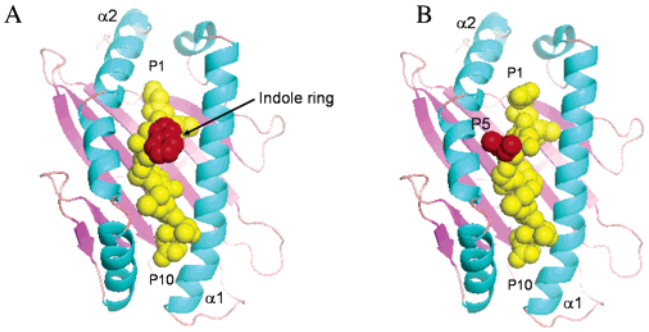

Figure 3. Space filling representations of **21** and ELA docked in the A6-TCR/Tax/HLA-A2 complex. ELA mimetic **21** (A) and ELA (B) viewed from above the HLA-A2 molecule. The α-helical domains of HLA-A2 are shown in blue, and its β-sheet floor is shown in magenta. Peptidic structures are shown in Corey−Pauling−Kultun representations (yellow) with their central P5 position in red. Both structures display a similar global binding mode with an identical orientation of their HLA-A2 anchoring side chains. The main difference resides in the orientation of the indole side chain of **21** as compared to that of I5 of ELA.

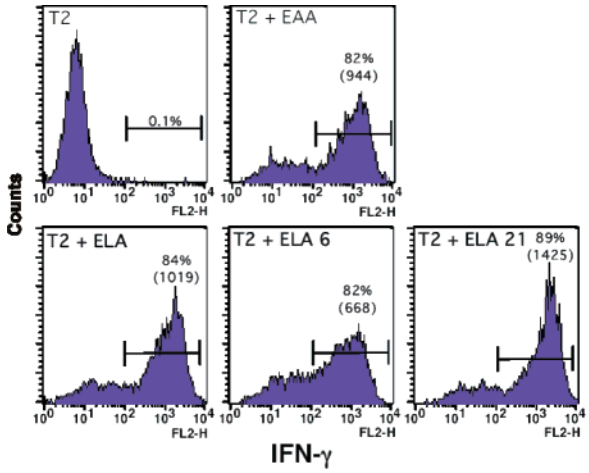

Figure 4. Melan-A/MART-1-specific clone Mel1-37 was stimulated for 6 h with T2 cells, pulsed with EAA, ELA, **6**, or **21** or without (as negative control). T-cells were fixed at the end of the stimulation, permeabilized, stained, and analyzed on a FACScan. Percentages of IFN-γ-labeled cells are indicated, as well as mean fluorescence intensities in parentheses.

of the seven clones tested. This compound was even capable of activating the clone MEL1-37 at a level superior to that reached with ELA, as shown by the significantly higher mean fluorescence intensity of T-cell clones stimulated by this peptidomimetic **21** (1425) than by ELA (1019) (Table 2 and Figure 4). It is worth noting that the HLA-A2 binding affinity of **21** is just about equal to that of ELA (Table 1). Therefore, the higher capacity of this analogue essentially relies on the TCR/peptidomimetic interaction. Although the fine characteristics of TCR/peptide interactions that condition T-cell activation and response remain unclear, Davies et al.[40,41] recently proposed, in their two-step model for T-cell recognition, that it is the final folding of the two CDR3 loops of the TCR over the antigenic peptide that is crucial for T-cell activation outcome. In the case of **21**, its docking study revealed a binding mode to the MHC class-I HLA-A2 molecule highly similar to that of ELA (Figures 2 and 3). The first step of T-cell recognition should therefore probably be identical for both the peptide ELA and its mimetic **21**. The capacity of **21** to induce stronger IFN-γ secretion than ELA could then be a consequence of stronger and/or more appropriate contacts of its indole acetyl side chain with the MEL1-37 TCR CDR3 loops. The fact that **18**, the analogue of **21** lacking the side chain carbonyl group, was unable to activate T-cell clones could be due to its higher flexibility, whereas the amide link of **21** could better constrain its indolic side chain to orient itself toward the TCR binding zone. In any event, these results and those obtained here with other peptidomimetics are new experimental illustrations to the fact that certain T-cells are very sensitive to even minor structural changes of the central part of their ligand. Nevertheless, this fine structural specificity is not a characteristic common to all T-cells. This is clearly illustrated by our observation that the CDM41-ELA1 PBL clone responded in a similar fashion to several ELA analogues (i.e., **6**, **7**, **10**, **11**, and **21**), all bearing polar aromatic units in their central part (i.e., indole, *p*-nitroxyphenyl and quinoline, Table 2). One might thus argue that the CDR3 loops of the CDM41-ELA1 receptor are flexible enough to accommodate sterically and electronically different organic motifs of the same general type during the second step of their recognition of these peptidomimetics.[42,43] In sharp contrast, one of the clones used in this study (i.e., 10C10) did not tolerate any of the alterations we performed on its ligand including the simple substitution of Ile at P5 by other standard aromatic residues (i.e., in **1** to **3**). Interestingly, another clone (M199.2.7) not tolerating either these simple modifications was, however, capable of recognizing the ELA mimetics **6** and **21**. This suggests that nonpeptidic alterations could be perhaps more efficient than peptidic ones

in generating active analogues of wild-type epitopes, as a plausible consequence of their higher structural diversity.

Conclusion

Replacing the central part of MHC class-I bound antigenic peptides (APs) by nonpeptidic residues is an approach to peptidomimetics that has previously been followed in attempts essentially aimed at increasing the binding affinity of the altered peptides to MHC molecules, while improving their bioresistance in applications in vivo. To the best of our knowledge, none of these modifications were specifically implemented with the possibility of altering and modulating TCR/peptide interactions in mind. The experimental findings described therein demonstrate the value of our LigandFit-based rational design of antigenic peptidomimetics in which the central part is replaced by a pseudo-peptidic unit that can be equipped with a side chain capable of interacting with the CDR3 loops of TCRs. Most of the 20 altered peptides, thus designed, retained or even exceeded the binding affinity of the parent ELA peptide to the MHC class-I HLA-A2 molecule. Furthermore, five of them (i.e., **6**, **7**, **10**, **11**, and **21**) were capable of inducing T-cell responses. The Melan-A-specific T-cell clones used in this study appeared particularly sensitive to polar aromatic side chains and, more especially, to indole-containing motifs. The two most potent compounds (i.e., **6** and **21**) feature such a motif. The most spectacular results of this study are those obtained with the second-generation peptidomimetic **21**. Although this heavily modified peptide structure is not the best HLA-A2 ligand of those we designed therein, it is capable of inducing IFN-γ secretion by one of the T-cell clones tested at a level higher than that reached by the already optimized analogue ELA peptide. This compound undeniably constitutes a valuable lead for the development of peptidomimetic-based vaccine-type immunotherapies against melanoma. Future work will address the pursuit of the immunological evaluation of this peptidomimetic and of its structural modification aimed at improving its bioresistance while maintaining or increasing its immunogenecity. Results will be reported in due course.

Experimental Section

Docking Methodology. All molecular modeling calculations were performed on a Silicon Graphics Octane workstation using Catalyst 4.7 and Cerius^2 4.7 molecular modeling softwares. The peptidomimetics used in this docking study are listed in Table 1. The following procedure was used to perform the docking study. First, the three-dimensional structure of the A6-TCR/Tax/HLA-A2 complex was taken from the PDB file 1A07.[21] The Tax ligand and all the water molecules were removed. Hydrogen atoms were added using the Cerius^2 templates for the protein residues. The 23 peptide analogue and mimetic structures were constructed in Catalyst. Partial charges were assigned using the Gasteiger method[44] as implemented in Cerius^2. A site model based on the Tax ligand docked into the protein was identified by LigandFit. Then, the docking[45] of the 23 ligands employed the following protocol: (a) a Monte Carlo conformational search for generating a candidate ligand conformation, (b) selection of a ligand position and orientation based on comparing the shape of the binding site model with that of the ligand conformation, and (c) evaluation of the goodness of docking by computing the dock energies using a grid-based energy calculation. The dock energy is expressed as the sum of the ligand internal strain energy and the interaction energy of the ligand with the protein. Then, the position and the orientation of the ligand are optimized by minimizing the dock energy, with respect to rigid body translations and rotations of the ligand using a steepest descent method. The docked conformations found are then clustered, and the first 20 are saved. A superimposition of the highest docked structure obtained for each peptidomimetic with the parental peptide structure from the 1A07 PDB file enables us to gain insight of the backbone modification consequence on the interaction with the protein.

Materials and Methods. All reagents were either purchased from Aldrich, Acros, or Fluka. Amino acids and their derivatives were purchased from Advanced Chem. Tech. (U.K.), Bachem, or Novabiochem (Switzerland). The Wang resin and HBTU were purchased from Novabiochem. All organic solvents were of analytical quality and Milli-Q (Millipore) water was used for reverse phase (RP) HPLC analyses and purifications. Peptide and peptidomimetic syntheses were performed manually in a glass reactor (vide infra). RP-HPLC analyses were performed on a Thermo system using a Chromolith performance RP-18e column (4.6 $\times$ 100 mm, 5 μm) with P1000 XR pumps at a flow rate of 3 mL min^{-1} (see Table 1 and Supporting Information). Semipreparative purifications were performed on the same Thermo system using a Waters semi-prep deltapack RP-C18 column (3.9 mm $\times$ 300 mm, 100 Å pore size, 15 μm). The mobile phase was composed of 0.1% (v/v) TFA/H_2O (Solvent A) and 0.1% TFA/CH_3CN (Solvent B). A gradient elution (0−40 min: 90% to 50% A) was applied at a flow rate of 4 mL min^{-1}. Column effluent was monitored by UV detection at 214 and 254 nm using a Thermo UV 6000 LP diode array detector. Flash column chromatography was carried out under positive pressure using 40−60 μm silica gel (Merck) and the indicated solvents. Evaporations were conducted under reduced pressure at temperatures less than 45 °C unless otherwise noted. Further drying of the residues was accomplished under high vacuum. NMR spectra of samples in the indicated solvent were run at 400 MHz on a Bruker DPX spectrometer. Electrospray ionization mass spectrometric low- and high-resolution data (ESIMS, HRMS) were obtained from the Mass Spectrometry Laboratory at the European Institute of Chemistry and Biology (IECB), Pessac, France, and from the Centre Régional de Mesures Physiques de l'Ouest (CRMPO), Université Rennes 1, Rennes, France.

***N*-*tert*-Butoxycarbonyl-1,2-diaminoethane (25).**[46] To an ice-cooled solution of 1,2-diaminoethane (**24**, 2.23 g, 30 mmol) in dry THF (30 mL) was added dropwise a solution of Boc_2O (1.96 g, 9 mmol) in THF (15 mL). The reaction mixture was stirred at 0 °C for 30 min, then at room temperature overnight. After evaporation of the solvent, the solid mixture was dissolved in ethyl acetate (200 mL) and washed with brine (3 $\times$ 30 mL). The organic layer was dried over Na_2SO_4, filtered, and evaporated to give **25** as a white solid (2.73 g, 97%): ^{1}H NMR (DMSO-d_6, 400 MHz) δ 1.38 (s, 9H), 2.53 (m, 2H), 2.91 (m, 2H), 6.75 (bs, 1H, NH); ^{13}C NMR (DMSO-d_6, 100 MHz) δ 156.5, 78.5, 44.2, 42.3, 28.1.

***N*-(*N*′-*tert*-Butoxycarbonyl-2-aminoethyl)glycine ethyl ester (26).**[47] To an ice-cooled solution of **25** (1 g, 6.25 mmol) and diisopropylethylamine (0.215 mL, 1.25 mmol) in dry THF (20 mL) was slowly added a solution of ethylbromoacetate (0.206 mL, 1.85 mmol) in dry THF (20 mL). The reaction mixture was stirred 1 h at 0 °C and then 3 h at room temperature. The mixture was then poured into brine and extracted with ethyl acetate (3 $\times$ 20 mL). The combined organic layers were washed again with brine, dried over Na_2SO_4, filtered, and evaporated to give a residue, which was submitted to flash column chromatography, eluting with CH_2Cl_2−MeOH (10:1), to furnish pure **26** as a colorless oil (0.26 g, 56%): ^{1}H NMR ($CDCl_3$, 400 MHz) δ 1.26 (t, J = 7.1 Hz, 3H), 1.44 (s, 9H), 2.83 (m, 2H), 3.27 (m, 2H), 3.46 (s, 2H), 4.19 (q, J = 7.1 Hz, 3H), 5.22 (bs, 1H, NH); ^{13}C NMR ($CDCl_3$, 100 MHz): 177.8, 161.2, 83.0, 65.5, 55.6, 53.9, 33.8, 19.7; ESIMS (positive mode): *m*/*z* (rel. intensity) 247 (MH^+, 100%).

***N*-Aloc-*N*-(*N*′-Fmoc-2-aminoethyl)glycine (27).**[48] To a solution of **26** (250 mg, 1.0 mmol) in a 2:3 water−dioxane solvent mixture (10 mL) and Na_2CO_3 (534 mg, 5.0 mmol) was added dropwise a solution of allylchloroformate (0.118 mL, 1.12 mmol) in dioxane (2 mL). This reaction mixture was stirred at room temperature for 90 min, after which time it was poured into water (5 mL) and extracted with ethyl acetate (2 $\times$ 20 mL). The combined organic layers were washed twice with 1 N HCl (10 mL) and brine (10 mL), dried over Na_2SO_4, filtered, and evaporated. The resulting

residue was then submitted to flash column chromatography, eluting with ethyl acetate−cyclohexane (1:1), to furnish the desired *N*-Aloc derivative of **26** as a colorless oil (242 mg, 76%): ^{1}H NMR ($CDCl_3$, 400 MHz) δ 1.28 (t, J = 7.0 Hz, 3H), 1.43 (s, 9H), 3.27 (m, 2H), 3.46 (t, J = 5.7, 2H), 3.97 (d, J = 6.4 Hz, 2H), 4.21 (m, 2H), 4.60 (dd, J = 5.4, 16.4 Hz, 2H), 5.35 (m, 2H), 5.90 (m, 1H); ^{13}C NMR ($CDCl_3$, 100 MHz) δ 170.5, 156.5, 133.0, 117.8, 67.0, 61.9, 50.3, 49.1, 39.7, 28.8, 14.6; HRMS (ESIMS, positive mode) calcd for $C_{13}H_{22}N_2O_6Na$ 325.1375, found 325.1367.

To a solution of the *N*-Aloc derivative of **26** (200 mg, 0.63 mmol) in THF (5 mL) was added a solution of LiOH (46 mg, 1.90 mmol) in water (5 mL). This mixture was stirred overnight at room temperature, evaporated to remove THF, and lyophilized. The resulting crude carboxylic acid was then dissolved in TFA (5 mL) and let standing without stirring for 30 min. After removal of TFA by evaporation, the resulting TFA salt was dissolved in water and treated with 1 N NaOH until pH 9. A solution of Fmoc-OSu (213 mg, 0.63 mmol) in CH_3CN (10 mL) was then added, and the mixture was stirred at room temperature overnight, after which time it was poured into water (20 mL) and extracted once with Et_2O (10 mL). The aqueous phase was acidified with 1 N HCl until pH 1 and extracted twice with CH_2Cl_2 (2 × 20 mL). The combined organic layers were washed twice with brine (2 × 10 mL), dried over Na_2SO_4, filtered, and evaporated to furnish **27** as a yellow powder (260 mg, 91%): IR ($CHCl_3$) 2360, 1697, 1540, 1474, 1450, 1141, 740 cm^{-1}; ^{1}H NMR ($CDCl_3$, 400 MHz) δ 3.15 (s, 2H), 3.32 (m, 2H), 3.92 (d, J = 12.7 Hz, 2H), 4.28 (d, J = 7.33 Hz, 2H), 4.49 (m, 2H), 4.83 (d, J = 6.0 Hz, 1H), 5.15 (m, 1H), 5.25 (m, 1H), 5.88 (m, 1H); ^{13}C NMR ($CDCl_3$, 100 MHz) δ 172.1, 170.6, 157.0, 144.7, 143.5, 141.6, 134.0, 128.8, 128.5, 128.2, 126.0, 125.8, 121.2, 121.0, 117.6, 66.2, 61.9, 49.7, 47.6, 46.8; ESIMS (positive mode) *m*/*z* (rel. intensity) 425.5 (MH^+, 48); HRMS (ESIMS, positive mode) calcd for $C_{23}H_{24}N_2O_6Na$ 447.1532, found 447.1537.

General Procedure for Solid-Phase Peptidomimetic Synthesis. The synthesis of all peptidomimetics and peptide fragments thereof was carried out on a Wang resin (0.89, 0.91, or 0.93 mmol/g) via standard SPPS protocols.[49] To a solution of *N*-Fmoc-Val-OH (10 equiv relative to resin loading) in dry CH_2Cl_2 (a few drops of DMF were required to ensure complete dissolution) under N_2 was added di-*iso*-propylcarbodiimide (DIC, 5 equiv). The reaction mixture was stirred for 20 min at 0 °C. In the meantime, the resin was suspended in dry CH_2Cl_2 and allowed to swell for 20 min. After filtration, the symmetrical *N*-Fmoc-Val anhydride solution and DMAP (0.1 equiv) were added, and the resin was shaken 4 h. After filtration, the resin was successively washed twice with DMF, MeOH, and CH_2Cl_2 and again DMF. The Fmoc protecting group was removed by using twice a solution of piperidine in DMF (1:4, v/v) for 3 min then for 7 min. After filtration, the resin was successively washed as before. The SPPS was then continued using *N*-Fmoc amino acids (3 equiv) or *N*-Fmoc-AMBA-OH (3 equiv) in the presence of HBTU (3 equiv) and DIEA (5 equiv) in DMF. Each coupling reaction was performed for 45 min, after which time the resin was washed as before. The last amino acid (i.e., Glu or βAla) was introduced as an *N*-Boc-protected residue. Completion of each coupling reaction was monitored via the trinitrobenzenesulfonic acid (TNBS) test. After final deprotection and cleavage from the resin, all compounds were checked for purity by RP-HPLC and purified by semipreparative RP-HPLC (see Materials and Methods). Compound identification was accomplished by ESIMS analysis in positive mode.

Formation of the Resin-Bound Peptidomimetics 4−6 by Reductive Amination on Solid Support. The ELA mimetics **4**−**6** were obtained by replacing one or two peptide bonds by the aminomethylene (CH_2-NH) surrogate. To the *N*-terminal α-amino group of the resin-bound peptide was added *N*-Fmoc-Gly-H (2.5 equiv relative to the resin loading) and $NaBH_3CN$ (7.5 equiv) in a solution of 1% (v/v) AcOH in DMF for 2 h, as previously described.[25] The completion of the reaction was monitored by the TNBS test. All coupling reactions that were performed after the introduction of a reduced peptide bond were carried out as described above.

Formation of the Resin-Bound Peptidomimetics 7−10 and 12−17 by *N*-Alkylation on Solid Support. To the free resin-bound glycine amine (Scheme 3) suspended in a solution of 2% (v/v) AcOH in DCE was added the appropriate aldehyde RCHO in a quantity sufficient to reach a concentration of 0.25 M in the reaction medium. After being mixed for 2 h, the reaction mixture was filtered, and a freshly prepared 0.25 M solution of $NaBH(OAc)_3$ in DCE was added and allowed to react for 3 h. The reaction mixture was then quenched with MeOH (3 times) and filtered, and the resin was washed twice with CH_2Cl_2, MeOH, and again CH_2Cl_2. The next reductive amination with the secondary amine anchored to the support was then carried out overnight under shaking by using a solution of *N*-Fmoc-Gly-H (10 equiv) and $NaBH_3CN$ (10 equiv) in a 1% AcOH−DMF solvent mixture. After filtration and washings with MeOH and CH_2Cl_2, the last coupling reactions were performed as before according to the general procedure described above. For the peptidomimetic **17**, the same procedure was applied except that the *N*-alkylation step was carried out overnight using phenylacetaldehyde (20 equiv) in the presence of $NaBH_3CN$ (20 equiv) in a solution of 1% AcOH in DMF.

Formation of the Resin-Bound Peptidomimetic 11. The construction of its peptide fragment was done as described above via standard SPPS protocols, and *N*-Aloc-*N*-(*N*′-Fmoc-2-aminoethyl)glycine (**27**, 3 equiv) was introduced using the coupling reagents HBTU (3 equiv) and DIEA (5 equiv). The resin-supported Aloc-containing peptide (see Scheme 4) was then treated at room temperature with $Pd(PPh_3)_4$ (0.1 equiv) and $PhSiH_3$ (20 equiv) in dry CH_2Cl_2 with occasional stirring for 20 min at room temperature. This deprotection step was repeated once. The completion of the Aloc group removal was controlled via the chloranil test. After filtration, the resin was washed twice with CH_2Cl_2, MeOH, and again CH_2Cl_2. To the resin (50 mg, 23 μmol) then suspended in a solution of 2% ACOH in DCE (2 mL) was added 4-hydroxybenzaldehyde (53.5 mg, 46 μmol, 20 equiv) and $NaBH(OAc)_3$ (93.5 mg, 46 μmol, 20 equiv). The resin was gently shaken overnight, and the reaction mixture was quenched three times with MeOH and washed twice with CH_2Cl_2, MeOH, and again CH_2Cl_2. The completion of this alkylation step was checked via the chloranil test.

Formation of the Resin-Bound Peptidomimetics 18 and 19. To the free resin-bound AMBA-derived primary amine (100 mg, 0.556 mmol, see Scheme 5) were added bromoacetic acid (111 mg, 0.80 mmol), as a 0.4 M solution in DMF, and DIC (0.156 mL, 1.0 mmol) as a 2.0 M solution in DMF. The resin was allowed to react in this media for 5 min, after which time the solution of reagents was drained, and the resulting brominated resin **28** was washed with DMF (5 × 5 mL). To this functionalized resin was then added a 1.0 M DMSO solution of either N^{in}-Boc-tryptamine (**29**, 260 mg, 1 mmol) or *O*-*t*Bu-tyramine (**30**, 193 mg, 1 mmol).[50] These mixtures were allowed to react for 3 h, after which time they were filtered and the resins were washed twice with DMF, MeOH, CH_2Cl_2, and again DMF (ca. 5 mL of each solvent), before being submitted to the same reductive amination conditions as those described for **7**−**10**, using *N*-Fmoc-Gly-H. The final amino acid coupling reactions were then performed as before according to the general SPPS procedure described above.

Formation of the Resin-Bound Peptidomimetics 20 and 21. The free resin-bound AMBA-derived primary amine (100 mg, 0.556 mmol see Scheme 6) was first coupled with Fmoc-Gly-OH using standard SPPS conditions according to the general procedure described above. After removal of the Fmoc-protecting group, the resulting free amine was condensed with Fmoc-Gly-H, under the same reductive amination conditions as those described for **4**−**6**, to furnish the AMBA-containing resin-bound *N*-Fmoc-aminoethyl glycine construct. Its free secondary amine function was then acylated with either indolacetic acid (101 mg, 0.56 mmol, 10 equiv) or phenylacetic acid (87 mg, 0.56 mmol, 10 equiv) in the presence of DIC (90 μL, 0.56 mmol, 10 equiv) in DMF (5 mL). The resin was shaken for 1 h, after which time the mixture was filtered and the resin was washed as before. Both acylation reactions were repeated once. The final amino acid coupling reactions were then

performed as before according to the general SPPS procedure described above.

Formation of the Resin-Bound Peptidomimetics 22 and 23. Peptidomimetics **22** and **23** were synthesized according to the general SPPS procedure described above, using either *N*-Fmoc-Tic-OH (3 equiv) or *N*-Fmoc-Tpi-OH (3 equiv). The introduction of the reduced peptide bond was performed again via condensation reactions with *N*-Fmoc-Gly-H (3 equiv) using $NaBH_3CN$ (10 equiv). These reactions were carried out overnight. The last coupling reactions were then performed as before according to the general SPPS procedure described above.

General Procedure for TFA Cleavage. Final deprotection and cleavage from the resin were carried out using a TFA−H_2O−TIS mixture (95:2.5:2.5) for 4 h, except for the indole-containing constructs **17** and **21**, for which EDT was added to the cleavage cocktail [i.e., TFA−H_2O−TIS−EDT (92.5:2.5:2.5:2.5)]. All the peptidomimetic constructs were then precipitated using cold Et_2O, filtered, dissolved in a water−acetonitrile−TFA mixture and lyophilized. They were then purified by semipreparative RP-HPLC (see Materials and Methods).

Cell Lines. The TAP-deficient human mutant cell line CEMx721 T2 (T2) used as presenting cell was a generous gift from T. Boon (Ludwig Institute for Cancer Research, Brussels, Belgium). The EBV-B-transformed cell line LAZ-338 used as feeder cell was a gift from T. Hercend (Vertex Pharmaceutical, Abingdon, England). These two cell lines were cultured in RPMI-1640 (Sigma-Aldrich, Saint Quentin Fallavier, France) containing 10% FCS (Biowest, Nuaille, France), penicillin-streptomycin (100U PEN/mL-100 μg STREP/mL (Sigma) and glutamine (1 nM) (Sigma).

T-Cell Clones. Melanoma-reactive CD8 T-cell clones (M77.84, M199.2.7, M199.3.2, 10C10, M17.29ELA1, MEL1.37, and CDM41ELA1), specific for Melan-A/MART-1 antigen, were obtained from TILs or from PBLs stimulated ex vivo by peptide pulsed antigen presenting cells (APC).[51] Melanoma-specific clones were expanded using a polyclonal T-cell stimulation protocol, as previously described.[52] Briefly, 2000 T-cell clones were distributed in 96-well plates with 150 μL of culture medium (RPMI with 8% human serum and IL-2 150 U/mL) and irradiated feeder cells: LAZ EBV-B cells (10^4/well) and allogenic PBLs (10^5/well). Polyclonal T-cell amplification was performed using 15 μg/mL of PHA-L (Sigma) at the onset of the culture. Culture medium was changed 2 days later to remove PHA-L and then twice a week. T-cell clones were split when their number exceeded 2×10^5/well.

HLA-A*0201 Binding Assay. The relative peptidomimetic binding capacity to HLA-A*0201 was assessed using the TAP-deficient HLA-$A2^+$ T2 cells. These cells were loaded with saturating concentrations (100 μM) of the different peptidomimetics and, in parallel, of the natural Melan-A/MART-1_{26-35} peptide (EAAGIGILTV) and of its peptide analogue A27L (ELAGIGILTV), with human β2-microglobulin (100 ng/mL, Sigma), by overnight incubation at 37 °C in serum-free medium (RPMI-1640). Cells were washed twice before staining with mouse mAb HB54 (HLA-A2 specific) (ATCC) to measure HLA-A2 Ag expression. Briefly, cells were stained with the specific or isotype control mAb for 30 min at 4 °C. After being washed, cells were incubated for 30 min with the secondary goat $F(ab')_2$ fragment anti-mouse IgG-PE (Beckman Coulter, Marseille, France) and analyzed on a FACScan flow cytometer using Cellquest software (Becton Dickinson, Grenoble, France). Increased fluorescence intensity, compared to fluorescence in the absence of peptide or peptidomimetic is expressed as the ratio fluorescence intensity (RFI) for HLA-A2 expression calculated as follows: mean fluorescence intensity with the specific mAb divided by mean fluorescence intensity with the negative control. This RFI correlates with the HLA-A2 binding affinity. The relative HLA-A2 affinity of each peptide analogue or peptidomimetic construct is expressed as the ratio between the RFI induced by the optimized analogue ELA and the tested peptide analogues and peptidomimetics. RFI ratios superior or inferior to 1 respectively indicate a higher or lower HLA-A2 binding affinity of the tested peptide analogues and peptidomimetics compared to that of ELA.

T-Cell Stimulation. T2 cells were incubated for 1 h at 37 °C in the presence of ELA analogues or mimetics (10 μM). After being washed, 2×10^5 peptide-pulsed T2 cells were incubated with 10^5 T-cell clones in 200 μL of RPMI-1640/10% FCS, in the presence of 10 μg/mL of brefeldin A (Sigma). The cultures were realized in round-bottom 96-well plates and incubated for 6 h at 37 °C in 5% CO_2 humidified atmosphere. Cells were then fixed 10 min at room temperature in a solution of PBS 4% paraformaldehyde (Electron Microscopy Sciences), washed, and stored at 4 °C until labeling.

Flow Cytometric Analysis of Intracellular IFN-γ. Stimulated T-cell clones were stained for IFN-γ using the method described by Jung and co-workers.[53] Briefly, fixed cells were washed in PBS containing 0.1% BSA and 0.1% saponin (Sigma) and stained for 30 min at room temperature with the PE-conjugated mouse anti-human IFN-γ MAb (BD Pharmingen) at a concentration of 5 μg/mL, which was shown to give optimal staining, and then washed twice. Reagent dilutions and washes were made with PBS containing 0.1% BSA and 0.1% saponin. After being stained, cells were resuspended in PBS and 1×10^4 events were analyzed on a FACScan flow cytometer using Cell Quest software (Beckton Dickinson). Results are expressed by the fraction of stimulated T-cells secreting IFN-γ and by the mean fluorescence intensity of IFNγ labeled cells which correlates with the intensity of clone activation.

Acknowledgment. Financial support from the University of Bordeaux 1 (Interdepartmental competitive grant, 2001−2004), the European Institute of Chemistry and Biology (Pessac, France, 2003−2005), and La Ligue Contre le Cancer (Labellisation 2002 and 2005) is gratefully acknowledged. The authors also thank the Conseil Régional d'Aquitaine for a postdoctoral fellowship for C.D.-C.

Supporting Information Available: ^1H and ^{13}C NMR spectra of compounds **25**−**27**, RP-HPLC chromatograms and low-resolution ESI^+ mass spectra of ELA peptide analogues **1**−**3** and peptidomimetics **4**−**23**, HPLC-determined purities of all analogues and peptidomimetics **1**−**23** (Table S1), and high-resolution mass spectrometric data and TOCSY-based ^1H NMR chemical shifts assignments of **21** (Table S2). This material is available free of charge via the Internet at http://pubs.acs.org.

References

(1) Kagi, D.; Hengartner, H. Different roles for cytotoxic T cells in the control of infections with cytopathic versus noncytopathic viruses. *Curr. Opin. Immunol.* **1996**, *8*, 472−477.
(2) Greenberg, P. D. Adoptive T cell therapy of tumors: mechanisms operative in the recognition and elimination of tumor cells. *Adv. Immunol.* **1991**, *49*, 281−355.
(3) Cresswell, P. Antigen processing and presentation. *Immunol. Rev.* **2005**, *205*, 5−7.
(4) Davis, M. M.; Boniface, J. J.; Reich, Z.; Lyons, D. S.; Hampl, J.; Arden, B.; Chien, Y. Ligand recognition by alpha beta T cell receptors. *Annu. Rev. Immunol.* **1998**, *16*, 523−544.
(5) (a) Larche, M.; Wraith, D. C. Peptide-based therapeutic vaccines for allergic and autoimmune diseases. *Nat. Med.* **2005**, *11*, 69−76. (b) Boon, T.; Coulie, P. G.; Van den Eynde, B. J.; van der Bruggen, P. Human T cell responses against melanoma. *Annu. Rev. Immunol.* **2006**, *24*, 175−208.
(6) Rosenberg, S. A.; Yang, J. C.; Restifo, N. P. Cancer immunotherapy: moving beyond current vaccines. *Nat. Med.* **2004**, *10*, 909−915.
(7) Starr, T. K.; Jameson, S. C.; Hogquist, K. A. Positive and negative T cell selection. *Annu. Rev. Immunol.* **2003**, *21*, 139−176.
(8) (a) Kawakami, Y.; Eliyahu, S.; Sakaguchi, K.; Robbins, P. F.; Rivoltini, L.; Yannelli, J. R.; Appella, E.; Rosenberg, S. A. Identification of the immunodominant peptides of the MART-1 human melanoma antigen recognized by the majority of HLA-A2-restricted tumor infiltrating lymphocytes. *J. Exp. Med.* **1994**, *180*, 347−352. (b) Coulie, P. G.; Brichard, V.; Van Pel, A.; Wölfel, T.; Schneider, J.; Traversari, C.; Mattei, E.; De Plaen, C.; Lurquin, J.; Szikora, P.; Renauld, J. C.; Boon, T. A new gene coding for a differentiation antigen recognized by autologous cytolytic T lymphocytes on HLA-A2 melanomas. *J. Exp. Med.* **1994**, *180*, 35−42.

(9) Valmori, D.; Fonteneau, J. F.; Maranon Lizana, C.; Gervois, N.; Liénard, D.; Rimoldi, D.; Jongeneel, C. V.; Jotereau, F.; Cerottini, J. C.; Romero, P. Enhanced generation of specific tumor-reactive CTL in vitro by selected Melan-A/MART-1 immunodominant peptide analogs. *J. Immunol.* **1998**, *160*, 1750−1758.

(10) Blanchet, J. S.; Valmori, D.; Dufau, I.; Ayyoub, M.; Nguyen, C.; Guillaume, P.; Monsarrat, B.; Cerottini, J. C.; Romero, P.; Gairin, J. E. A new generation of Melan-A/MART-1 peptides that fulfill both increased immunogenicity and high resistance to biodegradation: implication for molecular anti-melanoma immunotherapy. *J. Immunol.* **2001**, *167*, 5852−5861.

(11) Brinckerhoff, L. H.; Kalashnikov, V. V.; Thompson, L. W.; Yamshchikov, G. V.; Pierce, R. A.; Galavotti, H. S.; Engelhard, V. H.; Slingluff, C. L. Terminal modifications inhibit proteolytic degradation of an immunogenic MART-1_{27-35} peptide: Implications for peptide vaccines. *Int. J. Cancer* **1999**, *83*, 326−334.

(12) (a) Hin, S.; Bianco, A.; Zabel, C.; Jung, G.; Walden, P. Mimetics of a T cell epitope based on poly-N-acylated amine backbone structures induce T cells in vitro and in vivo. *J. Biol. Chem.* **2001**, *276*, 48790−48796. (b) Bianco, A.; Brock, C.; Zabel, C.; Walk, T.; Walden, P.; Jung, G. New synthetic non-peptide ligands for classical major histocompatibility complex class I molecules. *J. Biol. Chem.* **1998**, *273*, 28759−28765.

(13) Hofbauer, G. F.; Kamarashev, J.; Geertsen, R.; Boni, R.; Dummer, R. Melan A/MART-1 immunoreactivity in formalin-fixed paraffin-embedded primary and metastatic melanoma: frequency and distribution. *Melanoma Res.* **1998**, *8*, 337−343.

(14) Kawakami, Y.; Eliyahu, S.; Delgado, C. H.; Robbins, P. F.; Sakaguchi, K.; Appella, E.; Yannelli, J. R.; Adema, G. J.; Miki, T.; Rosenberg, S. A. Identification of a human melanoma antigen recognized by tumor-infiltrating lymphocytes associated with in vivo tumor rejection. *Proc. Natl. Acad. Sci.* **1994**, *91*, 6458−6462.

(15) Pittet, M. J.; Valmori, D.; Dunbar, P. R.; Speiser, D. E.; Lienard, D.; Lejeune, F.; Fleischhauer, K.; Cerundolo, V.; Cerottini, J. C.; Romero, P. High frequencies of naive Melan-A/MART-1-specific CD8+ T cells in a large proportion of human histocompatibility leukocyte antigen (HLA)-A2 individuals. *J. Exp. Med* **1999**, *190*, 705−716.

(16) Romero, P.; Gervois, N.; Schneider, J.; Escobar, P.; Valmori, D.; Pannetier, C.; Steinle, A.; Wolfel, T.; Lienard, D.; Brichard, V.; van Pel, A.; Jotereau, F.; Cerottini, J. C. Cytolytic T lymphocyte recognition of the immunodominant HLA-A*0201-restricted Melan-A/MART-1 antigenic peptide in melanoma. *J. Immunol.* **1997**, *159*, 2366−2374.

(17) Ruppert, J.; Sidney, J.; Celis, E.; Kubo, R. T.; Grey, H. M.; Sette, A. Prominent role of secondary anchor residues in peptide binding to HLA-A2.1 molecules. *Cell*, **1993**, *74*, 929−937.

(18) Sliz, P.; Michielin, O.; Cerottini, J. C.; Luescher, I.; Romero, P.; Karplus, M.; Wiley, D. C. Structures of two closely related but antigenically distinct HLA-A2/melanocyte-melanoma tumor-antigen peptide complexes. *J. Immunol.* **2001**, *167*, 3276−3284.

(19) (a) Ayyoub, M.; Zippelius, A.; Pittet, M. J.; Rimoldi, D.; Valmori, D.; Cerottini, J. C.; Romero, P.; Lejeune, F.; Lienard, D.; Speiser, D. E. Activation of human melanoma reactive CD8+ T cells by vaccination with an immunogenic peptide analog derived from Melan-A/melanoma antigen recognized by T cells-1. *Clin. Cancer Res.* **2003**, *9*, 669−677. (b) Lienard, D.; Rimoldi, D.; Marchand, M.; Dietrich, P. Y.; van Baren, N.; Geldhof, C.; Batard, P.; Guillaume, P.; Ayyoub, M.; Pittet, M. J.; Zippelius, A.; Fleischhauer, K.; Lejeune, F.; Cerottini, J. C.; Romero, P.; Speiser, D. E. Ex vivo detectable activation of Melan-A-specific T cells correlating with inflammatory skin reactions in melanoma patients vaccinated with peptides in IFA. *Cancer Immun.* **2004**, *4*, 1−19.

(20) (a) Rudolph, M. G.; Wilson, I. A. The specificity of TCR/pMHC interaction. *Curr. Opin. Immunol.* **2002**, *14*, 52−65. (b) Rudolph, M. G.; Stanfield, R. L.; Wilson, I. A. *Annu. Rev. Immunol.* **2006**, *24*, 419−466.

(21) Garboczi, D. N.; Ghosh, P.; Utz, U.; Fan, Q. R.; Biddison, W. E.; Wiley, D. C. Structure of the complex between human T-cell receptor, viral peptide and HLA-A2. *Nature* **1996**, *384*, 134−140.

(22) (a) Pinilla, C.; Martin, R.; Gran, B.; Appel, J. R.; Boggiano, C.; Wilson, D. B.; Houghten, R. A. Exploring immunological specificity using synthetic peptide combinatorial libraries. *Curr. Opin. Immunol.* **1999**, *11*, 193−202. (b) Rubio-Godoy, V.; Dutoit, V.; Zhao, Y.; Simon, R.; Guillaume, P.; Houghten, R.; Romero, P.; Cerottini, J. C.; Pinilla, C.; Valmori, D. Positional scanning-synthetic peptide library-based analysis of self- and pathogen-derived peptide cross-reactivity with tumor-reactive Melan-A-specific CTL. *J. Immunol.* **2002**, *169*, 5696−5707. (c) Pinilla, C.; Rubio-Godoy, V.; Dutoit, V.; Guillaume, P.; Simon, R.; Zhao, Y.; Houghten, R. A.; Cerottini, J. C.; Romero, P.; Valmori, D. Combinatorial peptide libraries as an alternative approach to the identification of ligands for tumor-reactive cytolytic T lymphocytes. *Cancer Res.* **2001**, *61*, 5153−5160. (d) Douat-Casassus, C.; Marchand Geneste, N.; Diez, E.; Aznar, C.; Picard, P.; Geoffre, S.; Huet, A.; Bourguet-Kondracki, M.-L.; Gervois, N.; Jotereau, F.; Quideau, S. Covalent modification of a melanoma-derived antigenic peptide with a natural quinone methide. Preliminary chemical, molecular modelling and immunological evaluation studies. *Mol. BioSyst.* **2006**, *2*, 240−249. (e) Gagnon, S. J.; Borbulevych, O. Y.; Davis-Harrison, R. L.; Turner, R. V.; Damirjian, M.; Wojnarowicz, A.; Biddison, W. E.; Baker, B. M. T cell receptor recognition via cooperative conformational plasticity. *J. Mol. Biol.* **2006**, *363*, 228−243.

(23) Venkatachalam, C. M.; Jiang, X.; Oldfield, T.; Waldman, M. LigandFit: a novel method for the shape-directed rapid docking of ligands to protein active sites. *J. Mol. Graph. Model.* **2003**, *21*, 289−307.

(24) (a) Apostolopoulos, V.; Yu, M.; Corper, A. L.; Li, W.; McKenzie, I. F.; Teyton, L.; Wilson, I. A.; Plebanski, M. Crystal structure of a non-canonical high affinity peptide complexed with MHC class I: a novel use of alternative anchors. *J. Mol. Biol.* **2002**, *318*, 1307−1316. (b) Apostolopoulos, V.; Yu, M.; Corper, A. L.; Teyton, L.; Pietersz, G. A.; McKenzie, I. F.; Wilson, I. A.; Plebanski, M. Crystal structure of a non-canonical low-affinity peptide complexed with MHC class I: A new approach for vaccine design. *J. Mol. Biol.* **2002**, *318*, 1293−1305. (c) Saper, M. A.; Bjorkman, P. J.; Wiley, D. C. Refined structure of the human histocompatibility antigen HLA-A2 at 2.6 Å resolution. *J. Mol. Biol.* **1991**, *219*, 277−319. (d) Hillig, R. C.; Coulie, P. G.; Stroobant, V.; Saenger, W.; Ziegler, A.; Hulsmeyer, M. High-resolution structure of HLA-A*0201 in complex with a tumour-specific antigenic peptide encoded by the MAGE-A4 gene. *J. Mol. Biol.* **2001**, *310*, 1167−1176.

(25) Quesnel, A.; Zerbib, A.; Connan, F.; Guillet, J. G.; Briand, J. P.; Choppin, J. Synthesis and antigenic properties of reduced peptide bond analogues of an immunodominant epitope of the melanoma MART-1 protein. *J. Pept. Sci.* **2001**, *7*, 157−165.

(26) (a) Calbo, S.; Guichard, G.; Bousso, P.; Muller, S.; Kourilsky, P.; Briand, J. P.; Abastado, J. P. Role of peptide backbone in T cell recognition. *J. Immunol.* **1999**, *162*, 4657−4662. (b) Stemmer, C.; Quesnel, A.; Prévost-Blondel, A.; Zimmermann, C.; Muller, S.; Briand, J. P.; Pircher, H. Protection against lymphocytic choriomeningitis virus infection induced by a reduced peptide bond analogue of the H-2Db-restricted CD8+ T cell epitope GP33. *J. Biol. Chem.* **1999**, *274*, 5550−5556. (c) Ayyoub, M.; Mazarguil, H.; Monsarrat, B.; Van den Eynde, B.; Gairin, J. E. A structure-based approach to designing non-natural peptides that can activate anti-melanoma cytotoxic T cells. *J. Biol. Chem.* **1999**, *274*, 10227−10234.

(27) (a) Krebs, S.; Lamas, J. R.; Rognan, D. Substituting nonpeptidic spacers for the T cell receptor-binding part of class I major histocompatibility complex-binding peptides. *J. Biol. Chem.* **1998**, *273*, 19072−19079. (b) Rognan, D.; Scapozza, L.; Folkers, G.; Daser, A. Rational design of nonnatural peptides as high-affinty ligands for the HLA-B*2705 human leukocyte antigen. *Proc. Natl. Acad. Sci.* **1995**, *92*, 753−747.

(28) (a) Nielsen, P. E. *Peptide Nucleic Acids: Protocols and Applications*; Horizon Scientific Press: Portland, U.K., 1999. (b) Baker, E. S.; Hong, J. W.; Gaylord, B. S.; Bazan, G. C.; Bowers, M. T. PNA/dsDNA complexes: site specific binding and dsDNA biosensor applications. *J. Am. Chem. Soc.* **2006**, *128*, 8484−8492.

(29) Guichard, G.; Zerbib, A.; Le Gal, F.-A.; Hoebeke, J.; Connan, F.; Choppin, J.; Briand, J.-P.; Guillet, J.-G. Melanoma Peptide MART-1(27-35.) Analogues with Enhanced Binding Capacity to the Human Class I Histocompatibility Molecule HLA-A2 by Introduction of β-Amino Acid Residue: Implications for Recognition by Tumor-Infiltrating Lymphocytes. *J. Med. Chem.* **2000**, *43*, 3803−3808.

(30) (a) Weerapana, E.; Imperiali, B. Peptides to peptidomimetics: towards the design and synthesis of bioavailable inhibitors of oligosaccharyl transferase. *Org. Biomol. Chem* **2003**, *1*, 93−99. (b) Qian, Y.; Blaskovich, M.; Saleem, M.; Seong, M.; Wathen, S. P.; Hamilton, A. D.; Sebti, S. M. Design and structural requirements of potent peptidomimetic inhibitors of p21ras farnesyltransferase. *J. Biol. Chem.* **1994**, *269*, 12410−12413. (c) Cristau, M.; Devin, C.; Oiry, C.; Chaloin, O.; Amblard, M.; Bernad, N.; Heitz, A.; Fehrentz, J.-A.; Martinez, J. Synthesis and biological evaluation of bombesin constrained analogues. *J. Med. Chem.* **2000**, *43*, 2356−2361. (d) Lunney, E. A.; Para, K. S.; Rubin, J. R.; Humblet, C.; Fergus, J. H.; Marks, J. S.; Sawyer, T. K. Structure-based design of a novel Series of nonpeptide ligands that bind to the pp60src SH2 domain. *J. Am. Chem. Soc.* **1997**, *119*, 12471−12476.

(31) Bolin, D. R.; Swain, A. L.; Sarabu, R.; Berthel, S. J.; Gillespie, P.; Huby, N. J.; Makofske, R.; Orzechowski, L.; Perrotta, A.; Toth, K.; Cooper, J. P.; Jiang, N.; Falcioni, F.; Campbell, R.; Cox, D.; Gaizband, D.; Belunis, C. J.; Vidovic, D.; Ito, K.; Crowther, R.; Kammlott, U.; Zhang, X.; Palermo, R.; Weber, D.; Guenot, J.; Nagy,

Z.; Olson, G. L. Peptide and peptide mimetic inhibitors of antigen presentation by HLA-DR class II MHC molecules. Design, structure-activity relationships, and X-ray crystal structures. *J. Med. Chem.* **2000**, *43*, 2135−2148.
(32) Nagy, A.; Armatis, P.; Cai, R. Z.; Szepeshazi, K.; Halmos, G.; Schally, A. V. Design, synthesis, and in vitro evaluation of cytotoxic analogs of bombesin-like peptides containing doxorubicin or its intensely potent derivative, 2-pyrrolinodoxorubicin. *Proc. Natl. Acad. Sci.* **1997**, *94*, 652−656.
(33) Douat, C.; Heitz, A.; Martinez, J.; Fehrentz, J. A. Synthesis of N-protected-amino aldehydes from their morpholine amide derivatives. *Tetrahedron Lett.* **2000**, *41*, 37−40.
(34) Shannon, S. K.; Peacock, M. J.; Kates, S. A.; Barany, G. Solid-phase synthesis of lidocaine and procainamide analogues using backbone amide linker (BAL) anchoring. *J. Comb. Chem.* **2003**, *5*, 860−868.
(35) Burkoth, T. S.; Fafarman, A. T.; Charych, D. H.; Connolly, M. D.; Zuckermann, R. N. Incorporation of unprotected heterocyclic side chains into peptoid oligomers via solid-phase submonomer synthesis. *J. Am. Chem. Soc.* **2003**, *125*, 8841−8845.
(36) Olivos, H. J.; Alluri, P. G.; Reddy, M. M.; Salony, D.; Kodadek, T. Microwave-assisted solid-phase synthesis of peptoids. *Org. Lett.* **2002**, *4*, 4057−4059.
(37) Uno, T.; Beausoleil, E.; Goldsmith, R. A.; Levine, B. H.; Zuckermann, R. N. New submonomers for poly N-substituted glycines (peptoids). *Tetrahedron Lett.* **1999**, *40*, 1475−1478.
(38) Kruijtzer, J. A. W.; Hofmeyer, L. J. F.; Heerma, W.; Versluis, C.; Liskamp, R. M. J. Solid-phase syntheses of peptoids using Fmoc-protected N-substituted glycines: The synthesis of (retro)peptoids of Leu-enkephalin and substance P. *Chem. Eur. J.* **1998**, *4*, 1570−1580.
(39) Fonteneau, J. F.; Le Drean, E.; Le Guiner, S.; Gervois, N.; Diez, E.; Jotereau, F. Heterogeneity of biologic responses of melanoma-specific CTL. *J. Immunol.* **1997**, *159*, 2831−2839.
(40) Wu, L. C.; Tuot, D. S.; Lyons, D. S.; Garcia, K. C.; Davis, M. M. Two-step binding mechanism for T-cell receptor recognition of peptide−MHC. *Nature* **2002**, *418*, 552−558.
(41) Krogsgaard, M.; Davis, M. M. How T cells "see" antigen. *Nature Immunol.* **2005**, *6*, 239−245.
(42) Reiser, J. B.; Darnault, C.; Gregoire, C.; Mosser, T.; Mazza, G.; Kearney, A.; Van der Merwe, P. A.; Fontecilla-Camps, J. C.; Housset, D.; Malissen, B. CDR3 loop flexibility contributes to the degeneracy of TCR recognition. *Nature Immunol.* **2003**, *4*, 241−247.
(43) Valmori, D.; Gervois, N.; Rimoldi, D.; Fonteneau, J. F.; Bonelo, A.; Lienard, D.; Rivoltini, L.; Jotereau, F.; Cerottini, J. C.; Romero, P. Diversity of the fine specificity displayed by HLA-A0201-restricted CTL specific for the immunodominant Melan-A/MART-1 antigenic peptide. *J. Immunol.* **1998**, *161*, 6956−6962.
(44) Gasteiger, J.; Marsili, M. A new model for calculating atomic charges in molecules. *Tetrahedron Lett.* **1978**, *19*, 3181−3184.
(45) Vieth, M.; Hirst, J. D.; Dominy, B. N.; Daigler, H.; Brooks, C. L. Assessing search strategies for flexible docking. *J. Comput. Chem.* **1998**, *19*, 1623−1631.
(46) (a) Krapcho, A. P.; Kuell, C. S. Mono-protected diamines N-tert-Butoxycarbonyl-α,ω-alkanediamines from α,ω-alkanediamines. *Synth. Commun.* **1990**, *20*, 2559−2564. (b) Kurtan, T.; Nesnas, N.; Li, Y.-Q.; Huang, X.; Nakanishi, K.; Berova, N. chiral recognition by CD-sensitive dimeric zinc porphyrin host. 1. chiroptical protocol for absolute configurational assignments of monoalcohols and primary monoamines. *J. Am. Chem. Soc.* **2001**, *123*, 5962−5973.
(47) (a) Aldrian-Herrada, G.; Rabié, A.; Wintersteiger, R.; Brugidou, J. Solid-phase synthesis of peptide nucleic acid (PNA) monomers and their oligomerization using disulphide anchoring linkers. *J. Pept. Sci.* **1998**, *4*, 266−281.
(48) Jackson, R. W.; Tabone, J. C.; Howbert, J. J. Identification of TNF-α inhibitors from a split-Pool library based on a tyrosine-proline peptidomimetic scaffold. *Biol. Med. Chem. Lett.* **2003**, *13*, 205−208.
(49) (a) Lloyd-Williams, P.; Albericio, F.; Giralt, E. *Chemical Approaches to the Synthesis of Peptides and Proteins*; CRC Press: Boca Raton, FL, 1997. (b) Chan, C.; White, P. D. *Fmoc Solid Phase Peptide Synthesis: a practical approach*; Oxford Press: New York, 2000.
(50) Uno, T.; Beausoleil, E.; Goldsmith, R. A.; Levine, B. H.; Zuckermann, R. N. New submonomers for poly N-substituted glycines (peptoids). *Tetrahedron Lett.* **1999**, *40*, 1475−1478.
(51) (a) Gervois, N.; Guilloux, Y.; Diez, E.; Jotereau, F. Suboptimal activation of melanoma infiltrating lymphocytes (TIL) due to low avidity of TCR/MHC-tumor peptide interactions. *J. Exp. Med.* **1996**, *183*, 2403−2407. (b) Vignard, V.; Lemercier, B.; Lim, A.; Pandolfino, M. C.; Guilloux, Y.; Khammari, A.; Rabu, C.; Echasserieau, K.; Lang, F.; Gougeon, M. L.; Dreno, B.; Jotereau, F.; Labarriere, N. Adoptive transfer of tumor-reactive Melan-A-specific CTL clones in melanoma patients is followed by increased frequencies of additional Melan-A-specific T cells. *J. Immunol.* **2005**, *175*, 4797−4805.
(52) Jotereau, F.; Pandolfino, M. C.; Boudart, D.; Diez, E.; Dreno, B.; Douillard, J. Y.; Muller, J. Y.; LeMevel, B. High-fold expansion of human cytotoxic T-lymphocytes specific for autologous melanoma cells for use in immunotherapy. *J. Immunother.* **1991**, *10*, 405−411.
(53) Jung, T.; Schauer, U.; Heusser, C.; Neumann, C.; Rieger, C. Detection of intracellular cytokines by flow cytometry. *J. Immunol. Methods* **1993**, *159*, 197−207.

JM0613368